Transactions of the Korean Nuclear Society Spring Meeting
Jeju, Korea, May 12-13, 2016

Measurements of Critical Heat Flux using Mass Transfer System

Seung-Hyun Hong and Bum-Jin Chung*
Department of Nuclear Engineering, Kyung Hee University
#1732 Deokyoung-daero, Giheung-gu, Yongin-si, Gyeonggi-do, 17104, Korea
**Corresponding author*: *bjchung@khu.ac.kr*

1. Introduction

Critical heat flux (CHF) measurement experiments have been carried out in an effort to assess the applicability of the IVR-ERVC (In-Vessel Retention-External Reactor Vessel Cooling) strategy. In a severe accident, the reactor vessel is heated by the decay heat from core melts and the outer surface of reactor vessel is cooled by the natural convection of water pool. When the heat flux increases, boiling will start. Further increase of the heat flux may result in the CHF, which is generated by the bubble combinations. The CHF means that the reactor vessel was separated with coolant and wall temperature is raised rapidly. It may damage the reactor vessel. Also the CHF indicates the maximum cooling capability of the system. Therefore, the CHF has been used as a criterion for the regulatory and licensing. This work tried to simulate the CHF using a mass transfer system. The mass transfer experiment is a copper sulfate and sulfuric acid ($CuSO_4$- H_2SO_4) electroplating system.

2. Background studies

2.1 Study of IVR-ERVC

In order to assess the IVR-ERVC capability of AP1000, 2D experiments were performed using ULPU at the University of California [1]. The Penn State University [2] performed SBLB experiments for 1/20 scale of APR1400. The CEA [3] performed the CHF studies as forced boiling heat transfer called SULTAN experiments. KAIST [4] and Seoul National University [5] performed CHF experiments for scale down test facilities for APR1400. The measured CHF values showed similar trend and lied in the range of 1.6 MW/m^2 – 2.3 MW/m^2.

2.2 Critical heat flux mechanism

The increase in heat flux or surface temperature causes the boiling phenomena on the heated area. From the beginning of boiling region, nucleate boiling, the heat transfer is enhanced by buoyancy effect. However, in the high heat flux or wall temperature, liquid layer is separated with heated surface at due to the bubble combinations. Therefore the maximum heat flux region called CHF were observed.

While a number of methodologies for generating CHF has been proposed recently, it has not yet been precisely elucidated. Nowadays, the Hydrodynamic instability model by Zuber, and Liquid macrolayer dryout model by Haramura and Katto are the most widely recognized to explained the CHF phenomena. The Hydrodynamic instability model[6] was describe both Taylor instability which explained the location of vapor columns at regular intervals and Helmholtz instability which took place the collapsing on the vapor columns. The Liquid macrolayer dryout model[7] assumes that there is a certain thickness composed of the liquid stem between bubble and heated surface. In the high heat flux, when the dryout velocity on the vapor stem is higher than the departing velocity of the bubbles, the vapor columns are collapsed and combined with each other. According to those theories the film boiling is occurred.

3. Experimental methodology

3.1 Anology

A heat-transfer problem can be solved by mass-transfer experiments based on the analogy concept, as the mathematical models dealing with the two phenomena are the same [8]. Therefore, heat-transfer experiments can be replaced by mass-transfer experiments, and vice versa. In the present work, measurements were made using a sulfuric acid – copper sulfate (H_2SO_4–$CuSO_4$) electroplating system. This technique has been developed by several investigators and has become well established as an experimental methodology [9-12].

3.2 Boiling current technique

The point that can be calculated the heat transfer coefficient is called limiting current density was existed as shown in Fig 1. The limiting current are role of sensible heat transfer. After the limiting current, the hydrogen bubbles departed from the cathode electrode surface that are similar with the boiling phenomena on heat transfer system. Thus the boiling current region can be substitute the latent heat transfer. The more current density departed the more bubbles can causes the film boiling mechanism by bubble mergence on cathode surface. The main idea of this study is to simulate the CHF phenomena using the reduced hydrogen bubbles on the cathode surface.

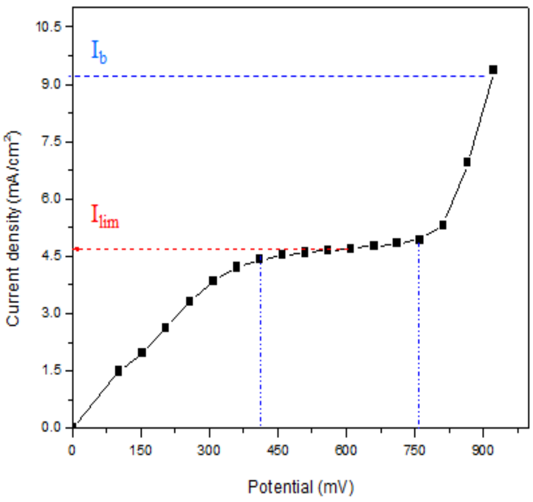

Fig. 1 Typical limiting current density curve.

4. Experiments apparatus

Figure 2 presents the electrical circuit. It was consisted of an open top acrylic tank, an anode and a cathode that was made of copper. The size of acrylic tank is of width 0.4m, height 0.2m, and length 0.4m to satisfy with the condition of pool boiling. The sulfuric acid concentration and the copper sulphate concentration were 1.5M and 0.05M respectively. The Prandtl number was 2,014. The anode width and length are 1.0×10^{-1} m, 2.0×10^{-1} m respectively. The cathode width and length are 1.0×10^{-2} m. The size of cathode was determined as 5 times of the most dangerous wavelength that do not affect the heater size. The equation of the most dangerous wavelength shows at Eq. (1).

$$\lambda_d = \sqrt{\frac{3\sigma}{g(\rho_l - \rho_v)}} \quad (1)$$

The σ is working fluid surface tension, ρ_v is vapor density of hydrogen, ρ_l is working fluid density, and g is gravitational acceleration. The calculation of electric potential was applied by a power supply (SGI DC Power supply SGI-100A/150V) and the current was measured by data acquisition (Agilent-34972A). By using a high current and voltage, the shunt resistor was used.

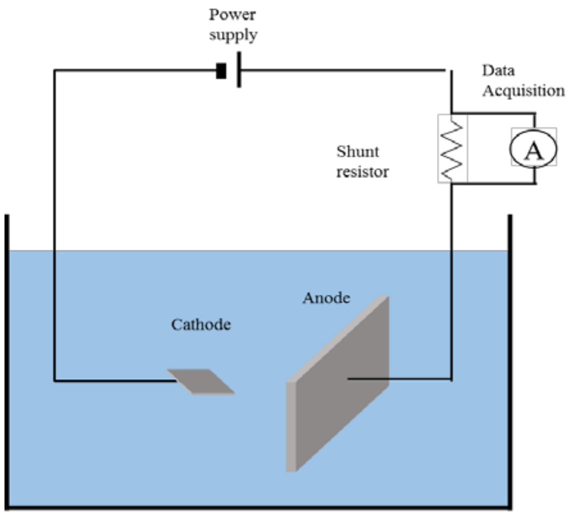

Fig. 2 Electrical circuit.

5. Results and Discussion

5.1 Visualization of CHF by mass transfer

The visualization results that performed by Westwater et al. to compare between heat and mass transfer is shown at Fig. 3[13]. The visualization of nucleate boiling region and film boiling region are similar with heat transfer results. Thus, the electroplating system in mass transfer can be deemed to simulate the CHF phenomena sufficiently.

	Heat transfer	**Mass transfer**
Nucleate boiling		
Film boiling		

Fig. 3 Comparison of CHF phenomena by visualization results

5.2 Comparison experimental results with CHF correlations

To fit the experimental conditions, such as IVR-ERVC, downward facing plate as angle dependent experiments of CHF were performed. The conditions of each study were different such as the experiments methods. Thus, the relative values were rather than the absolute values to compare. The study by Vishnevv was consistent with the experiments results.

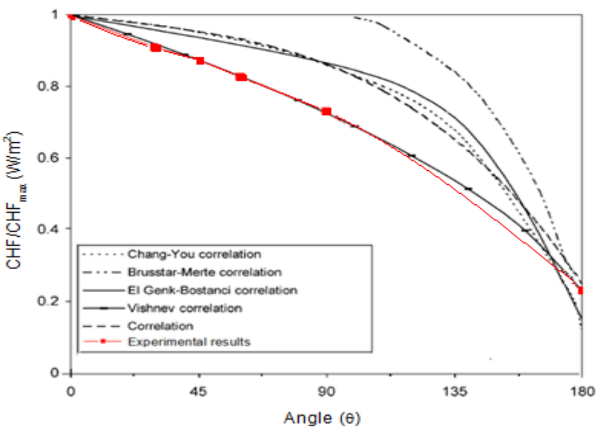

Fig. 4 Comparison the measurement CHF of angle dependent experiments with existing correlations.

5.3 Angle dependent results

The results of absolute value for the downward facing experiments was shown in Fig. 5. The higher angle has the higher CHF value. Because the fluid velocity is increased while the hydrogen bubbles had risen to the upper according to increase the angle. When the horizontal downward facing plate, the CHF was taken very low value due to the hydrogen bubbles in the vicinity was trapped on the electrode surface not to rise to the upper side. As the angle increases, since it increase the speed of the bubbles by acceleration that can be seen that linearly increased until 180° of the flat plate.

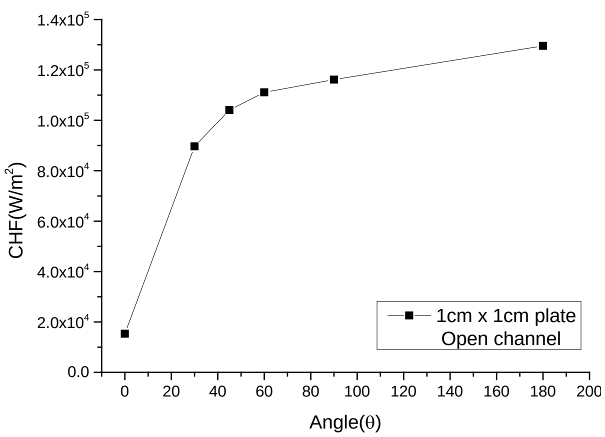

Fig. 5 The results of CHF as angle dependent on open channel single plate

5.4 CHF results by mass transfer calculation

The absolute value of CHF was calculated as shown in equation (3). The current density that shows the departed energy of the hydrogen on the electrodes was employed.

$$q''_{max} = \frac{I_b}{nF} \times M(H_2O) \times h_{fg} \times \sqrt{\frac{\rho_{H_2O}}{\rho_{H_2}}} \qquad (3)$$

The number of electrons in charge transfer reaction, n is 2, faraday constant, F is 96485 C/mole, molecular weight of H_2O is 18g/mole, latent heat is h_{fg} = 2247.63 J/g, vapor density of H_2O ρ_{H_2O} is 0.5956 kg/m^3, and vapor density of hydrogen ρ_{H_2} is 0.0813 kg/m^3. Only the current density was measured value. To found the difference between heat and mass transfer results, the horizontal upward facing experiments was selected. The calculation of experimental results is 169.16 kW/m^2.

5.5 CHF results by heat transfer correlation

The CHF correlation that was created by Zuber [15] and was fixed by Kutateladze [16] was used to estimate as applying to the property of sulfuric acid and copper sulfate.

$$q''_{max} = C h_{fg} \rho_v^{1/2} [\sigma g(\rho_l - \rho_v)]^{1/4} \qquad (2)$$

When the C is Constant number for finite flat plate, $h_{fg}$is Latent heat, σ is working fluid surface tension, ρ_v is vapor density of hydrogen, $\rho_l$is working fluid density, and g is gravitational acceleration. The calculation results of CHF correlation is 472.71 kW/m^2.

5.6 Comparison both of results

Comparing the results between the CHF correlation and experiments result can be found the similarities both of them. Because the condition of those properties were applied to same as each calculations. The relative error between these two sets of data was 64 %. The differences for each calculation were anticipated due to the characteristic factors. As a results, if the affecting factors are studied continuously, the similarity of those calculations will be able to prove as the same value.

6. Conclusions

The experiments of simulations as heat transfer CHF phenomena were carried out using the mass transfer system. Mechanism of hydrogen vapor bubbles generated and combined can be simulated water bubbles mechanism. And also the both heat and mass transfer mechanism of CHF can be identified in the same methods. Therefore, the CHF phenomena can be simulated enough by mass transfer.

ACKNOWLEGEMENT

This study was sponsored by the Ministry of Science, ICT and Future Planning (MSIP) and was supported by Nuclear Research & Development program grant funded by the National Research Foundation (NRF) (Grant Code: 2014M2A8A1030777).

REFERENCES

[1] T. N. Dinh, J. P. Tu, and T. G. Theofanous, Two-Phase Natural Circulation Flow in AP-1000 In-Vessel Retention-Related ULPU-V Facility Experiments, Proceedings of ICAPP'04, Pittsburgh, PA USA, June pp. 13-17, 2004.

[2] F. B. Cheung, J. Yang, M. B. Dizon, J. L. Rempe, K. Y. Suh, and S. B. Kim, On the Enhancement of External Reactor Vessel Cooling of High-Power Reactors, NURETH-10, Seoul, Korea, October pp.5-9, 2003.

[3] S. Rouge, I. Do, and G. Geffraye, Reactor Vessel External Cooling for Corium Retention SULTAN Experimental Program and Modeling with CATHARE Code, Workshop Proceedings on In-Vessel Core Debris Retention and Coolability, NEA/CSNI/R(98)18, Garching, Germany, March pp.3-6, 1988.

[4] Y. H. Jeong, S. H. W. P. Baek, Critical heat flux experiments on the reactor vessel wall using 2-D slice test section, Nuclear Technology, 152, pp.162-169, 2005.

[5] B. H Bae, Development of Optimized Reactor Insulator for Severe Accident Mitigation of APR1400, TR.A06NS04.S2009.150, KOREA HYDRO & NUCLEAR POWER CO., LTD, 2009

[6] Zuber, Hydrodynamic aspects of boiling heat transfer, AEC report, AECU-4439, Physics and Mathematics, 1959.

[7] A. Bejan, Convection Heat Transfer, 3rd ed., John Wiley & Sons, INC, New York, pp.207-210, 2003.

[8] H. S. Ahn, M. H. Kim, Visualization study of critical heat flux mechanism on a small and horizontal copper heater, International Journal of Multiphase Flow, 41, pp.1-12 (2012).

[9] V. G. Levich, Physicochemical Hydrodynamics, Prentice Hall, Englewood Cliffs, NJ, 1962.

[10] J. N. Agar, Diffusion and convection at electrodes, Discussion of Faraday Society, 26, 1, pp.27-37, 1947.

[11] C. W. Tobias and R. G. Hickman, Ionic mass transfer by combined free and forced convection, Zeitschrift für Physikalische Chemie, 229, pp. 145-166, 1965.

[12] E. J. Fenech, C. W. Tobias, Mass transfer by free convection at horizontal electrodes, Electrochimica Acta, 2, pp.311-325, 1960.

[13] J.W. Westwater, S. Yilmaz, Heat Transfer, 102, 26, 1980.

[14] A. Priarone, Effect of surface orientation on nucleate boiling and critical heat flux of dielectric fluids, International Journal of Thermal Sciences, 44, pp.822-831, 2005.

[15] Zuber, N., Trans. ASME, 80, 711, 1958.

[16] Kutateladze, S.S., Kotloturbostroenie, 3, 10, 1948.